

NUMERICAL ANALYSIS OF VAPOR FLOW IN A HORIZONTAL CYLINDRICAL HEAT PIPE

Mr. Selah M. Salih
Automobile Tech. Eng. Dept.
Technical College - Najaf

Mr. Qahtan A. Abed
Automobile Tech. Eng. Dept.
Technical College - Najaf

Mr. Dhafeer M. AL-Shamkhi
Automobile Tech. Eng. Dept.
Technical College - Najaf

ABSTRACT

The steady two-dimensional flow of a horizontal heat pipe in vapor region is investigated numerically. For study of heat transfer and fluid flow behaviors of the heat pipe, the governing equations in vapor region have been solved using a finite difference method. The numerical results of heat transfer and fluid flow are presented for Reynolds numbers ranging of ($Re = 4, 10$), the Prandtl number taken is ($Pr=0.00368$), and the pipe dimension is taken to be ($L/R = 5$). The results show that the stream function at the wall increases linearly in the evaporator, decreases linearly in the condenser and is steady in the adiabatic region because of uniform inflow and outflow boundary conditions. Also, it can be seen that as the Reynolds number increases, the pressure distributions shift up without considerable change in their shapes. The numerical analysis have shown that for the low and moderate Reynolds number, the shear stress becomes zero at a point very close to the end of the condenser. For verification of current model, the results of stream function for a heat pipe have been compared with the previous study at the same boundary conditions and a good agreement has been noticed.

KEYWORDS—Vapor region; heat pipe; numerical study.

التحليل العددي لجريان البخار في انبواب حراري افقي اسطواني

م.م. ظافر مائع حاجم
قسم هندسة تقنيات السيارات
الكلية التقنية - نجف

م.م. فحطان عدنان عبد
قسم هندسة تقنيات السيارات
الكلية التقنية - نجف

م.م. صلاح مهدي صالح
قسم هندسة تقنيات السيارات
الكلية التقنية - نجف

الخلاصة:

تم إجراء دراسة عددية لجريان مائع مستقر ثنائي البعد في انبواب حراري افقي لمنطقة البخار. من اجل دراسة سلوك انتقال الحرارة وجريان المائع في الانبواب الحراري. استخدمت طريقة الفروق المحددة لحل المعادلات الحاكمة لمنطقة البخار. تم تمثيل النتائج العددية لمعادلات انتقال الحرارة لعدد رينولدز في المدى ($Re = 4, 10$)، إخذ عدد برانتل ($Pr=0.00368$)، وابعاد الانبواب إخذت بنسبة ($L/R = 5$). النتائج بينت ان قيم دالة الجريان عند الجدار تزداد للمبخر وتقص للمكثف بشكل خطي ومستقرة للمنطقة المعزولة حرارياً بسبب الظروف الحدية المتجانسة لمنطقة الدخول والخروج. كذلك لوحظ عند زيادة عدد رينولدز، ان توزيع الضغط يرتفع بدون حدوث تغيير كبير بإشكاله. النتائج العددية بينت لعدد رينولدز

الواطيء والمعتدل ، ان اجهاد القص اصبح صفرا" عند نقطة قريبة جدا" لنهاية المكثف. وللتحقق من النموذج الحالي، تم مقارنة النتائج العددية لدالة الجريان مع دراسة سابقة عند نفس الظروف الحدية وكانت مقبولة.

NOMENCLATURE

C_p = heat capacity at constant pressure (kj/kg. K)
 h_{fg} = latent heat of vaporization (kj/kg)
 k = thermal conductivity (W/m. K)
 L = length (m)
 P = pressure (N/m²)
 Q = heat transfer (W)
 R = gas constant (kj/kg. K)
 rv = Vapor radius (m)
 ro =outer radius of pipe (m)
 Re = Reynolds number
 Pr = prandtl number
 T = temperature (K)
 v = radial vapor velocity (m/sec)
 u = axial velocity (m/sec)
 V = reference velocity (m/sec)
 x = axial coordinate (m)
 r = redial coordinate (m)

Greek Symbols

Ψ = stream function (m²/sec)
 ω = vorticity (sec⁻¹)
 α = fluid thermal diffusivity (m²/sec)
 ν = kinematics viscosity (m²/sec)
 μ = dynamic viscosity (kg/m. sec)
 ρ = density (kg/m³)
 τ = shear stress (N/m²)
 θ = dimensionless temperature

Subscripts

* = dimensionless term
 a =adiabatic
 c =condenser
 e = evaporator
 v = vapor
 int = interface
 o = outer
 sat = saturated

INTRODUCTION

The heat pipe is a vapor-liquid phase-change device that transfers heat from a hot reservoir to a cold reservoir using capillary forces generated by a wick or porous material and a working fluid. Heat pipes are the most effective passive method of transferring heat available today. Heat pipes can transmit heat at high rates and have a very high thermal conductance.

Heat pipes have been applied to a wide variety of thermal processes and technologies. Heats pipes have been applied in the cooling devices include generators, motors, nuclear, heat collection

from exhaust gases, solar and geothermal energy. In general, heat pipes have advantages over many traditional heat-exchange devices, (Doran, 1989).

The vapor flow in heat pipes has been investigated by various authors, (Rajashree and Sankara, 1990), (Chan and Faghri, 1995), (Zhu and Vafai, 1999), and (Kim et al, 2003) have published many techniques, theories, and experimental investigations of different heat pipe structures. They found the pressure and velocity distributions along the heat pipe depended on the value of radial Reynolds numbers.

(Nouri-Borujerdi and Layeghi, 2004) analyzed the vapor flow in concentric annular heat pipe using SIMPLE algorithm and staggered grid scheme. They found the flow and heat for vapor heat pipe was affected by increasing of radial Reynolds numbers.

(Yau, 2007) studied an 8-row thermosyphon-based heat pipe heat exchanger for tropical building HVAC systems experimentally. This research was an investigation into how the sensible heat ratio (SHR) of the 8-row HPHE was influenced by each of three key parameters of the inlet air state, namely, dry-bulb temperature, and relative humidity and air velocity.

(David et al., 2008) design and test of a pressure controlled heat pipe (PCHP), testing showed that (PCHP) was capable of maintaining a stable evaporator temperature within (0.1K) despite wide swings in heat load and heat sink temperature.

In this paper a numerical model has been used for analysis of vapor flow in heat pipe operation. The steady state incompressible flow has been solved in cylindrical coordinates in vapor region. The governing equations have been solved using finite difference with collocated grid scheme. The objective of this paper is study the heat transfer and fluid flow behavior of a conventional heat pipe operation.

MATHEMATICAL MODEL AND GOVERNING EQUATIONS

Figure 1 shows the simplified model and the coordinate system of the constant conductance heat pipe (CCHP) used in the present study. The heat pipe configuration can be divided into three radial regions, namely, vapor space, wick region and wall region. The working fluid is saturated with wick in liquid phase. The power applied to the heater in evaporator causes the liquid in the wick to vaporize. The vapor flows to the condenser section and releases the heat as it condenses. The released heat is rejected through the wall to the ambient. The condensed working fluid in the wick returns to heater section by the capillary force of the wick structure. To analysis the behavior of flow of fluid and heat through the heat pipe by using continuity, momentum and energy equations as flows.

Heat applied to evaporator section by an external source is conducted through the pipe wall and wick structure, where it vaporizes the working fluid. The resulting vapor pressure drives the vapor through the adiabatic section to the condenser, where the vapor condenses and releasing its latent heat of vaporization to the provided heat sink. The capillary pressure created by the wick structure, pumps the condensed fluid back to the evaporator. Therefore, the heat pipe can continuously transport the latent heat of vaporization from the evaporator to the condenser sections. This process will continue as long as there is sufficient capillary pressure to drive the condensate back to the evaporator.

At the vapor-wick interface, the temperature is assumed to be saturated, corresponding to interface pressure during heat pipe operation. Axial conduction along the wall and wick is assumed negligible.

The steady state two-dimensional incompressible laminar flow with constant viscosity in cylindrical (r - x) coordinate, and no heat generation. The governing equations in vapor region are continuity, Navier-Stokes and energy equations, (Rajashree and Sankara, 1990), are given as follows:

$$\frac{\partial u}{\partial x} + \frac{1}{r} \frac{\partial(rv)}{\partial r} = 0 \quad (1)$$

$$\rho u \frac{\partial u}{\partial x} + \rho v \frac{\partial u}{\partial r} = -\frac{\partial p}{\partial x} + \mu \left[\frac{\partial^2 u}{\partial x^2} + \frac{1}{r} \frac{\partial u}{\partial r} + \frac{\partial^2 u}{\partial r^2} \right] \quad (2)$$

$$\rho u \frac{\partial v}{\partial x} + \rho v \frac{\partial v}{\partial r} = -\frac{\partial p}{\partial r} + \mu \left[\frac{\partial^2 v}{\partial x^2} + \frac{1}{r} \frac{\partial v}{\partial r} + \frac{\partial^2 v}{\partial r^2} - \frac{v}{r^2} \right] \quad (3)$$

$$\rho c p \left[u \frac{\partial T}{\partial x} + v \frac{\partial T}{\partial r} \right] = K \left[\frac{\partial^2 T}{\partial x^2} + \frac{1}{r} \frac{\partial T}{\partial r} + \frac{\partial^2 T}{\partial r^2} \right] \quad (4)$$

The radial velocities at liquid-vapor interface, (Borujerdi, 2004), as following:

$$\begin{cases} v_e = +\frac{Q_e}{2\pi R_o L_e \rho_v h_{fg}} \\ v_a = 0 \\ v_c = -\frac{Q_c}{2\pi R_o L_c \rho_v h_{fg}} \end{cases} \quad (5)$$

The temperature at the vapor-liquid interface of the evaporator and condenser is calculated approximately using Clausius-Clapeyron equation, (Borujerdi, 2004):

$$T_{\text{int}} = T(x, r_v) = \frac{1}{\frac{1}{T_{\text{sat}}} - \frac{R}{h_{fg}} \ln \frac{P_v(T_v)}{P_{\text{sat}}(T_{\text{sat}})}} \quad (6)$$

The boundary conditions for vapor region are as following, (Rajashree and Sankara, 1990).

At both pipe ends are:

$$v = u = 0 \quad \frac{\partial T}{\partial x} = 0 \quad (7)$$

At pipe centerline the symmetry boundary conditions are:

$$v = 0, \quad \frac{\partial u}{\partial r} = 0 \quad \& \quad \frac{\partial T}{\partial r} = 0 \quad (8)$$

Pressure gradient at the wall at a particular time is calculated from the momentum equation and it is given by:

$$\frac{\partial p}{\partial x} = \frac{2}{\text{Re}} \left[\frac{1}{r} \frac{\partial u}{\partial r} + \frac{\partial^2 u}{\partial r^2} \right] - 2v \frac{\partial u}{\partial r} \quad (9)$$

The shear rate is also calculated from the equation:

$$\tau = \frac{2}{\text{Re}} \frac{\partial u}{\partial r} \quad (10)$$

METHOD OF SOLUTION

The governing equations are discretized using a finite difference approach and the equations are solved using upwind difference method with collocated grid scheme as shown in Fig.2. For the numerical analysis, it is convenient to use the governing equations in stream function and vorticity function:

$$ru = \frac{\partial \psi}{\partial r} \quad (11)$$

$$rv = -\frac{\partial \psi}{\partial x} \quad (12)$$

$$\omega = \frac{\partial v}{\partial x} - \frac{\partial u}{\partial r} \quad (13)$$

Using these and eliminating pressure the governing equations are transformed to

$$-\omega = \frac{1}{r^2} \frac{\partial^2 \psi}{\partial x^2} + \frac{1}{r^2} \frac{\partial^2 \psi}{\partial r^2} - \frac{1}{r^3} \frac{\partial \psi}{\partial r} \quad (14)$$

$$\frac{1}{r} \left[\frac{\partial \psi}{\partial r} \frac{\partial \omega}{\partial x} - \frac{\partial \psi}{\partial x} \frac{\partial \omega}{\partial r} \right] = \nu \left[\frac{\partial^2 \omega}{\partial x^2} + \frac{\partial^2 \omega}{\partial r^2} + \frac{3}{r} \frac{\partial \omega}{\partial r} \right] \quad (15)$$

$$\frac{1}{r} \left[\frac{\partial \psi}{\partial r} \frac{\partial T}{\partial x} - \frac{\partial \psi}{\partial x} \frac{\partial T}{\partial r} \right] = \alpha \left[\frac{\partial^2 T}{\partial x^2} + \frac{\partial^2 T}{\partial r^2} + \frac{1}{r} \frac{\partial T}{\partial r} \right] \quad (16)$$

Now, to make the governing equations form in non-dimensional and the boundary conditions using the following dimensionless quantities:

$$x_* = \frac{x}{r_v} \quad ; \quad r_* = \frac{r}{r_v} \quad ; \quad u_* = \frac{u}{V} \quad ; \quad v_* = \frac{v}{V} \quad ; \quad \psi_* = \frac{\psi}{V r_v} \quad (17)$$

$$\omega_* = \frac{\omega r_v}{V}; \quad p_* = \frac{p}{\frac{1}{2} \rho V^2}; \quad \theta = \frac{T}{T_o - T_s}; \quad pr = \frac{cp \mu}{k}; \quad \text{Re} = \frac{V r_v}{\nu}$$

By substitution the above dimensionless quantities, in the governing equation of motion yields:

$$-\omega_* = \frac{1}{r_*^2} \frac{\partial^2 \psi_*}{\partial x_*^2} + \frac{1}{r_*^2} \frac{\partial^2 \psi_*}{\partial r_*^2} - \frac{1}{r_*^3} \frac{\partial \psi_*}{\partial r_*} \tag{18}$$

$$\frac{1}{r_*} \left[\frac{\partial \psi_*}{\partial r_*} \frac{\partial \omega_*}{\partial x_*} - \frac{\partial \psi_*}{\partial x_*} \frac{\partial \omega_*}{\partial r_*} \right] = \frac{1}{\text{Re}} \left[\frac{\partial^2 \omega_*}{\partial x_*^2} + \frac{\partial^2 \omega_*}{\partial r_*^2} + \frac{1}{r_*} \frac{\partial \omega_*}{\partial r_*} + \frac{\omega_*}{r_*^2} \right] \tag{19}$$

if

$$\frac{1}{r_*} \left[\frac{\partial \psi_*}{\partial r_*} \frac{\partial \theta}{\partial x_*} - \frac{\partial \psi_*}{\partial x_*} \frac{\partial \theta}{\partial r_*} \right] = \frac{1}{\text{Re Pr}} \left[\frac{\partial^2 \theta}{\partial x_*^2} + \frac{\partial^2 \theta}{\partial r_*^2} + \frac{1}{r_*} \frac{\partial \theta}{\partial r_*} \right] \tag{20}$$

A finite-difference technique is applied to solve the governing equations. These three equations Eqs.(18), (19), and (20) are to be solved in a given region subject to the condition that the values of the stream function, temperature, and the vorticity, or their derivatives, are prescribed on the boundary of the domain.

Eq.(18) can be approximated using central – difference at the representative interior point (i, j) , then it can be written for regular mesh as:

$$\begin{aligned} \psi_*(i, j) = & [(\psi_*(i+1, j) + \psi_*(i-1, j))(\Delta r^2) + (\psi_*(i, j+1) + \psi_*(i, j-1))(\Delta x_*^2) - ((\Delta x_*^2 \Delta r_*^2) / (2r_*(j))) \\ & (\psi_*(i, j+1) + \psi_*(i, j-1)) + (\Delta x_*^2 \Delta r_*^2 r_*(j)^2) \omega_*(i, j)] / [2(\Delta r_*^2 + \Delta x_*^2)] \end{aligned} \tag{21}$$

Also, a central – difference formulation can be used for Eqs.(19), and (20). It is known that such a formulation may not be satisfactory owing to the loss of diagonal dominance in the sets of difference equations, with resulting difficulties in convergence when using an iterative procedure.

A forward – backward technique can be introduced to maintain the diagonal dominance coefficient of $(\omega_{i,j})$ in Eq.(19) and $(\theta_{i,j})$ in Eq.(20) which determines the main diagonal elements of the resulting linear system; this technique is outlined as follows (Najdat,1987):

Set; $B_1 = \psi_{i+1,j}^* - \psi_{i-1,j}^*$ and $B_2 = \psi_{i,j+1}^* - \psi_{i,j-1}^*$

Then approximate Eq.(19) by:

$$\frac{1}{r_*} \left[\frac{B_2}{2\Delta r_*} \frac{\partial \omega_*}{\partial x_*} - \frac{B_1}{2\Delta x_*} \frac{\partial \omega_*}{\partial r_*} \right] = \frac{1}{\text{Re}} \left[\frac{\partial^2 \omega_*}{\partial x_*^2} + \frac{\partial^2 \omega_*}{\partial r_*^2} + \frac{3}{r_*} \frac{\partial \omega_*}{\partial r_*} \right]$$

Now, if

$$B_1 \geq 0, \frac{\partial f}{\partial r} = \frac{f_{i,j+1} - f_{i,j}}{\Delta r} \quad , , , \quad B_1 < 0, \frac{\partial f}{\partial r} = \frac{f_{i,j} - f_{i,j-1}}{\Delta r}$$

if $B_2 \geq 0, \frac{\partial f}{\partial x} = \frac{f_{i,j} - f_{i-1,j}}{\Delta x}, \dots, B_2 < 0, \frac{\partial f}{\partial x} = \frac{f_{i+1,j} - f_{i,j}}{\Delta x}$

where, (f) refers to ω_*, θ_*

To assure the diagonal dominance of the coefficient matrix for $(\omega_{i,j}^*)$ and $(\theta_{i,j})$, which depends on the sign of (B_1) and (B_2) , Eqs (19) and (20) are expressed in the following difference forms:

For $B_1 \geq 0,$ and $B_2 \geq 0$

$$\omega_*(i, j) = [(\Delta x_*^2 + \frac{B_1 \Delta x_* \Delta r_* \text{Re}}{2r_*} + \frac{3\Delta x_*^2 \Delta r_*}{r_*})\omega_*(i, j+1) + (\Delta r_*^2 + \frac{B_2 \Delta x_* \Delta r_* \text{Re}}{2r_*})\omega_*(i-1, j) + (\Delta r_*^2)\omega_*(i+1, j) + (\Delta x_*^2)\omega_*(i, j-1)] / [2(\Delta x_*^2 + \Delta r_*^2) + \frac{3\Delta x_*^2 \Delta r_*}{r_*} + \frac{(B_1 + B_2)\Delta x_* \Delta r_* \text{Re}}{2r_*}] \tag{22a}$$

For $B_1 \geq 0,$ and $B_2 < 0$

$$\omega_*(i, j) = [(\Delta x_*^2 + \frac{B_1 \Delta x_* \Delta r_* \text{Re}}{2r_*} + \frac{3\Delta x_*^2 \Delta r_*}{r_*})\omega_*(i, j+1) + (\Delta r_*^2 - \frac{B_2 \Delta x_* \Delta r_* \text{Re}}{2r_*})\omega_*(i+1, j) + (\Delta r_*^2)\omega_*(i-1, j) + (\Delta x_*^2)\omega_*(i, j-1)] / [2(\Delta x_*^2 + \Delta r_*^2) + \frac{3\Delta x_*^2 \Delta r_*}{r_*} + \frac{(B_1 - B_2)\Delta x_* \Delta r_* \text{Re}}{2r_*}] \tag{22b}$$

For $B_1 < 0,$ and $B_2 \geq 0$

$$\omega_*(i, j) = [(\Delta x_*^2 - \frac{B_1 \Delta x_* \Delta r_* \text{Re}}{2r_*} - \frac{3\Delta x_*^2 \Delta r_*}{r_*})\omega_*(i, j-1) + (\Delta r_*^2 + \frac{B_2 \Delta x_* \Delta r_* \text{Re}}{2r_*})\omega_*(i-1, j) + (\Delta r_*^2)\omega_*(i+1, j) + (\Delta x_*^2)\omega_*(i, j+1)] / [2(\Delta x_*^2 + \Delta r_*^2) - \frac{3\Delta x_*^2 \Delta r_*}{r_*} + \frac{(B_2 - B_1)\Delta x_* \Delta r_* \text{Re}}{2r_*}] \tag{22c}$$

For $B_1 < 0,$ and $B_2 < 0$

$$\omega_*(i, j) = [(\Delta x_*^2 - \frac{B_1 \Delta x_* \Delta r_* \text{Re}}{2r_*} - \frac{3\Delta x_*^2 \Delta r_*}{r_*})\omega_*(i, j-1) + (\Delta r_*^2 - \frac{B_2 \Delta x_* \Delta r_* \text{Re}}{2r_*})\omega_*(i+1, j) + (\Delta r_*^2)\omega_*(i-1, j) + (\Delta x_*^2)\omega_*(i, j+1)] / [2(\Delta x_*^2 + \Delta r_*^2) - \frac{3\Delta x_*^2 \Delta r_*}{r_*} + \frac{(-B_1 - B_2)\Delta x_* \Delta r_* \text{Re}}{2r_*}] \tag{22d}$$

Dimensionless energy equation by using upwind finite difference:

For $B_1 \geq 0$, and $B_2 \geq 0$

$$\theta_*(i, j) = [(\Delta x_*^2 + \frac{B_1 \Delta x_* \Delta r_* \text{ Re Pr}}{2r_*} + \frac{\Delta x_*^2 \Delta r_*}{r_*})\theta_*(i, j+1) + (\Delta r_*^2 + \frac{B_2 \Delta x_* \Delta r_* \text{ Re Pr}}{2r_*})\theta_*(i-1, j) + (\Delta r_*^2)\theta_*(i+1, j) + (\Delta x_*^2)\theta_*(i, j-1)] / [2(\Delta x_*^2 + \Delta r_*^2) + \frac{\Delta x_*^2 \Delta r_*}{r_*} + \frac{(B_1 + B_2)\Delta x_* \Delta r_* \text{ Re Pr}}{2r_*}] \tag{23a}$$

For $B_1 \geq 0$, and $B_2 < 0$

$$\theta_*(i, j) = [(\Delta x_*^2 + \frac{B_1 \Delta x_* \Delta r_* \text{ Re Pr}}{2r_*} + \frac{\Delta x_*^2 \Delta r_*}{r_*})\theta_*(i, j+1) + (\Delta r_*^2 - \frac{B_2 \Delta x_* \Delta r_* \text{ Re Pr}}{2r_*})\theta_*(i+1, j) + (\Delta r_*^2)\theta_*(i-1, j) + (\Delta x_*^2)\theta_*(i, j-1)] / [2(\Delta x_*^2 + \Delta r_*^2) + \frac{\Delta x_*^2 \Delta r_*}{r_*} + \frac{(B_1 - B_2)\Delta x_* \Delta r_* \text{ Re Pr}}{2r_*}] \tag{23b}$$

For $B_1 < 0$, and $B_2 \geq 0$

$$\theta_*(i, j) = [(\Delta x_*^2 - \frac{B_1 \Delta x_* \Delta r_* \text{ Re Pr}}{2r_*} - \frac{\Delta x_*^2 \Delta r_*}{r_*})\theta_*(i, j-1) + (\Delta r_*^2 + \frac{B_2 \Delta x_* \Delta r_* \text{ Re Pr}}{2r_*})\theta_*(i-1, j) + (\Delta r_*^2)\theta_*(i+1, j) + (\Delta x_*^2)\theta_*(i, j+1)] / [2(\Delta x_*^2 + \Delta r_*^2) - \frac{\Delta x_*^2 \Delta r_*}{r_*} + \frac{(B_2 - B_1)\Delta x_* \Delta r_* \text{ Re Pr}}{2r_*}] \tag{23c}$$

For $B_1 < 0$, and $B_2 < 0$

$$\theta_*(i, j) = [(\Delta x_*^2 - \frac{B_1 \Delta x_* \Delta r_* \text{ Re Pr}}{2r_*} - \frac{\Delta x_*^2 \Delta r_*}{r_*})\theta_*(i, j-1) + (\Delta r_*^2 - \frac{B_2 \Delta x_* \Delta r_* \text{ Re Pr}}{2r_*})\theta_*(i+1, j) + (\Delta r_*^2)\theta_*(i-1, j) + (\Delta x_*^2)\theta_*(i, j+1)] / [2(\Delta x_*^2 + \Delta r_*^2) - \frac{\Delta x_*^2 \Delta r_*}{r_*} + \frac{(-B_1 - B_2)\Delta x_* \Delta r_* \text{ Re Pr}}{2r_*}] \tag{23d}$$

The corresponding boundary conditions at both ends of the heat pipe which are the no slip condition for the velocity and adiabatic condition for temperature.

$$\text{at } x_* = 0 \quad ; \quad \psi_*(0, r_*) = 0 \quad ; \quad \frac{\partial \theta}{\partial x_*} = 0 \tag{24}$$

$$\text{at } x_* = \frac{L}{r_v} \quad ; \quad \psi_*\left(\frac{L}{r_v}, r_*\right) = 0 \quad ; \quad \frac{\partial \theta}{\partial x_*} = 0$$

At the centerline, the symmetry conditions are applied.

$$\text{at } r_* = 0 \quad ; \quad \psi_*(x_*, 0) = 0 \quad ; \quad \frac{\partial \theta}{\partial r_*} = 0 \quad (25)$$

At the vapor –wick interface:

$$\text{at } r_* = 1 \quad ; \quad \psi_*(x_*, 1) = r_v \int_0^{x_*} \frac{Q}{2\pi L e \rho_v h_{fg}} dx_* \quad (26)$$

According to the coordinate system shown in **figure 1**, stream function $\psi_*(x_*, r_*)$ is negative in evaporator and positive in the condenser while in adiabatic regain is zero, (**Borujerdi, 2004**).

$$\theta(x_*, 1) = \frac{1}{[T_o - T_s] \left[\frac{1}{T_{sat}} - \frac{R}{h_{fg}} \ln \frac{P_v(T_v)}{P_{sat}(T_{sat})} \right]} \quad (27)$$

The solution procedure of the discretized equations is based on a line-by-line iteration method in the axial and radial directions using FORTRAN program. The sequence of numerical steps based on upwind difference is as follows:

1. Initialize the velocity, pressure, shear rate and temperature fields

$(u_*, v_*, P_*, \tau_*, \theta)$.

2. Solve Eqs.(11) and (12) for u and v .

3. Solve Eq. (9) for P .

4. Solve Eq. (10) for τ .

5. Solve Eq. (20) for θ .

6. Check Eq. (28) for convergence, if it is satisfied, calculations will be ended. Otherwise, replace $(u_*, v_*, P_*, \tau_*, \theta)$ and return to step (2) and repeat the above procedure until convergence is achieved.

The accuracy of the numerical solution is checked first by summation of the absolute value of the relative errors should be equal or less than (10^{-4}) . Second, the spot value should approach a constant value. The relative error (Err) in the numerical procedure is defined as, (**Borujerdi, 2004**):

$$Err = \sum_{cells} \left| \frac{\phi^{n+1} - \phi^n}{\phi^{n+1}} \right| \leq 10^{-4} \quad (28)$$

where superscript (n) refers to the previous iteration and term (ϕ) refers to ($\phi = u, v, P, \tau, \theta$).

A cylindrical heat pipe with water as working fluid is selected, in which the length of the evaporator is the same as the length of the condenser and a comparatively long adiabatic section is considered. The pipe dimensions are taken to be ($L/R = 5$), increment in space coordinates are ($\Delta x = 0.05$) and ($\Delta r = 0.1$). The computation is done for a mesh (101×11), Reynolds number (4 and 10), and the Prandtl number taken is ($Pr = 0.00368$). In the present analysis, the axial conduction along the heat pipe wall is neglected. The evaporator is maintained at constant temperature over its entire length and the condenser is cooled uniformly and is also kept at constant temperature.

RESULTS AND DISCUSSION

A computer program has been developed for predicting the stream function, radial and axial velocities, and temperature, pressure, and shear rate fields of vapor flow along the copper-water heat pipe. Using this program, a symmetric heat addition and rejection conditions are observed, as shown in **Fig.1**.

The stream function **Fig.3** at the wall increases linearly in the evaporator, decreases linearly in the condenser and is steady in the adiabatic region because of uniform inflow and outflow boundary conditions. From the axial variation of temperature graph **Fig.4** it is found that the temperature increases in the evaporator section, decreases in the condenser section, and the minimum temperature occurs in the condenser region. As the temperature in the evaporator increases, the vapor density in this section also increases and molecular mean free path becomes small compared to the vapor core diameter. Because of the vapor condenses and releasing its latent heat of vaporization to the provided heat sink.

When the Reynolds number is small, the streamlines are in the direction of increasing axial distance and the axial velocity component is positive everywhere with a transition to zero value occurring in a thin layer at the walls which is observed from **Fig.5**. The axial velocity profile becomes fully developed in a short distance and stays parabolic all along the length of the heat pipe. Because of the length of evaporator and condenser section is equal, and then the two quantities of evaporation and condensation of vapor are equal.

Also the radial velocity is negative in the evaporator section, zero in adiabatic section and positive in the condenser section, because of the flow direction is assumed negative of downward and positive of upward direction, as shown in **Fig.6**.

Figure 7 illustrates the pressure distribution along the heat pipe space centerline for various Reynolds numbers. It can be seen that as the Reynolds number increases, the pressure distributions shift up without considerable change in their overall shapes. As the Reynolds number increases the pressure in the condenser section is more recovered. The pressure distribution in the adiabatic section is a straight line similar to poiseuille flow results, while the profiles in the evaporator and condenser section demonstrate the effects of pressure head absorbed or created by evaporation or condensation, Due to the small pressure drop along the heat pipe at evaporator and condenser sections.

The shear rate as shown in **Fig.8** is found to be symmetric. Similar pattern follows for pressure distribution and the decrease in vapor pressure occurs smoothly in evaporator section, remains steady in the adiabatic section and then increases smoothly in the condenser section because of uniform inflow and outflow boundary conditions are equal.

The numerical analysis have shown that for the Reynolds number ($Re=4, 10$), the shear stress becomes zero at a point very close to the end of the condenser. However, as the Reynolds number increases, the flow reversal point moves backward toward the adiabatic section. Under this condition, the reversed flow region extends from the flow reversal point to the end of the condenser.

To verify our numerical solution we have recovered the heat pipe. A computer code, developed in the present work based on the FORTRAN language, has been validated using the results based on similar problem with those reported by (**Rajashree and Sankara, 1990**), as shown in **Fig.9** shows stream function comparison with previous study. This demonstrates that the present numerical analysis a good agreement for predicting the stream function distribution at Reynolds number ($Re=4$).

CONCLUSION

A numerical study is investigated the flow, temperature, velocity, pressure, and shear stress distributions for a horizontal heat pipe based on the obtained results in the present study, finding are:

- 1- At low and moderate Reynolds numbers, the present analysis predicts very small vapor temperature drop along the heat pipe. Due to the small pressure drop along the heat pipe.

- 2- The results show the stream function at the wall increases linearly in the evaporator, decreases linearly in the condenser and is steady in the adiabatic region because of uniform inflow and outflow boundary conditions.
- 3- Also, it can be seen that as the Reynolds number increases, the pressure distributions shift up without considerable change in their shapes.
- 4- The numerical analysis have shown that for the low and moderate Reynolds number, the shear stress becomes zero at a point very close to the end of the condenser.
- 5- The results have been compared with the available numerical data which have been done in the literature and have shown a good agreement.

REFERENCES

- [1] F.Doran, 1989, "Heat pipe research and development in the Americas," Heat Recovery Systems and CHP, Vol.9, pp.67-100.
- [2] R.Rajashree and K. Sankara, 1990, " A numerical Study of the Performance of Heat Pipe," Indian J. pure appl. Math, 21(1), pp: 95-108.
- [3] M. M. Chan and A. Faghri, 1995, "An Analysis of The Vapor Flow and Heat Conduction Through The Liquid Wick and Pipe Wall in a Heat Pipe With Single or Multiple Heat Sources," Int. J. Heat Mass Transfer, Vol. 33, No. 9, pp. 194.
- [4] N. Zhu and K. Vafai, 1999, "Analysis of Cylindrical Heat Pipe Incorporating the Effect of Liquid-Vapor Coupling and Non-Darcian Transport-A Closed form Solution," Int. J. Heat Mass Transfer, Vol. 42, pp. 3405- 3418.
- [5] S. J. Kim, J. K. Seo and K. H. Do, 2003, "Analytical and Experimental Investigation on the Operational Characteristics and Thermal Optimization of a Miniature Heat Pipe with a Grooved Wick Structure," Int. J. Heat Mass Transfer, Vol. 46, pp. 2051-2063.
- [6] A. Nouri-Borujerdi and M. Layeghi, , 2004, "Numerical Analysis of Vapour Flow in Concentric Annular Heat Pipes," Transaction of ASME: Journal of Heat Transfer, Vol. 126, pp. 442-448.
- [7] Y. H. Yau , 2007, "Application of a heat pipe heat exchanger to dehumidification enhancement in a HVAC system for tropical climates – a baseline performance characteristics study," International Journal of Thermal sciences , Vol. 46, pp.164 -171.
- [8] David B. Sarraf, Sanjida Tamanna, and Peter M. Dussinger, 2008, "pressure controlled heat pipe for precise temperature control," Space Technology and Applications International, American Institute of Physics, pp. 3-11.
- [9] A. Nouri-Borujerdi , 2004 "A Numerical Analysis of Vapor Flow in Concentric Annular Heat Pipes," Transaction of ASME: Journal of Fluids Engineering, Vol. 126, pp.442- 448.
- [10] Najdat N., 1987 "Laminar Flow Separation in Constructed Channel", Ph.D. Thesis, Michigan State University.

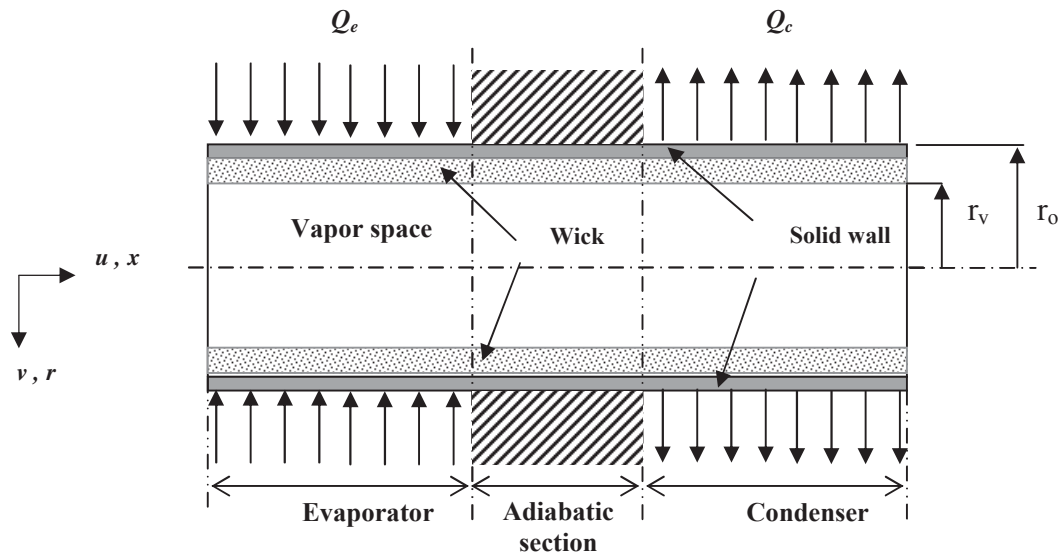


Fig. (1) Schematic of a cylindrical heat pipe

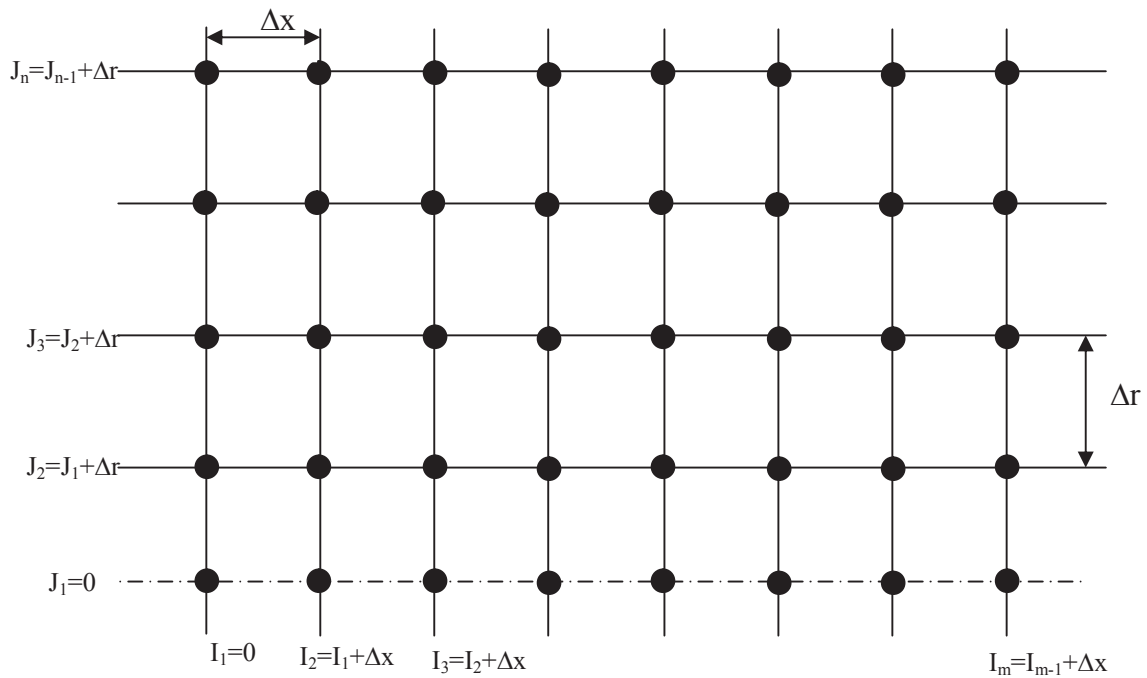


Fig.(2) The discretized domain

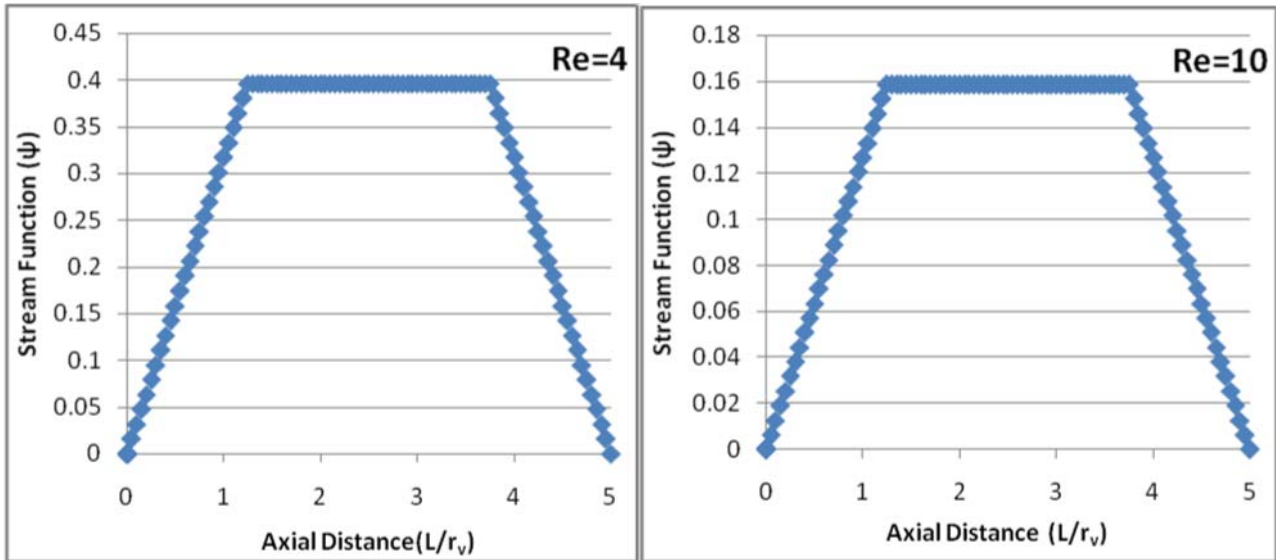


Fig. (3) Distribution of stream function at the wall a) $Re = 4$ b) $Re = 10$

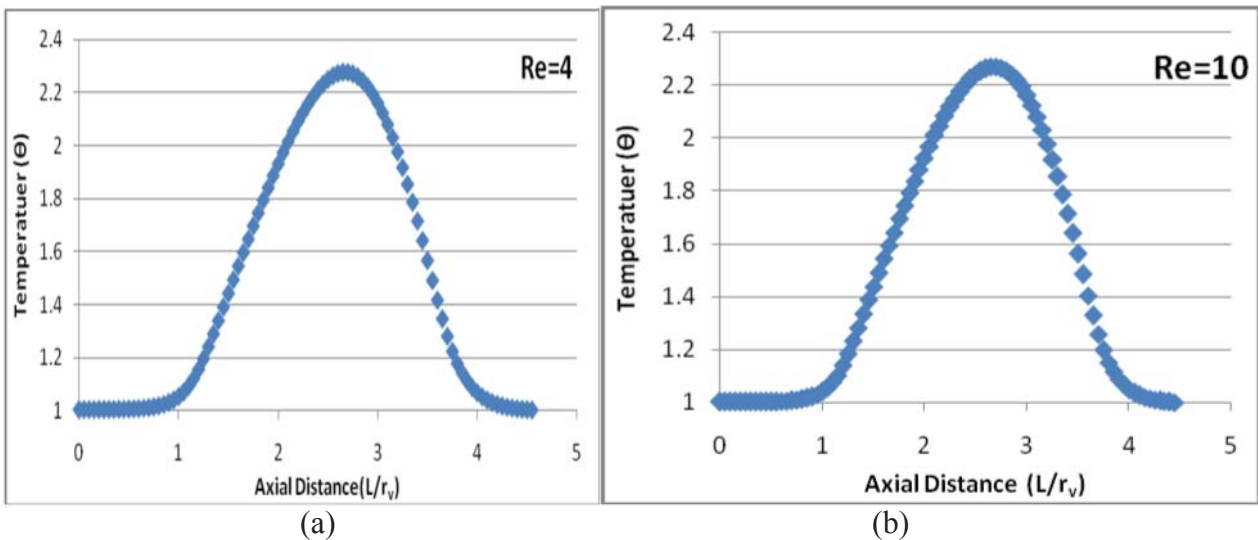


Fig. (4) Distribution of temperature near the wall a) $Re = 4$ b) $Re = 10$

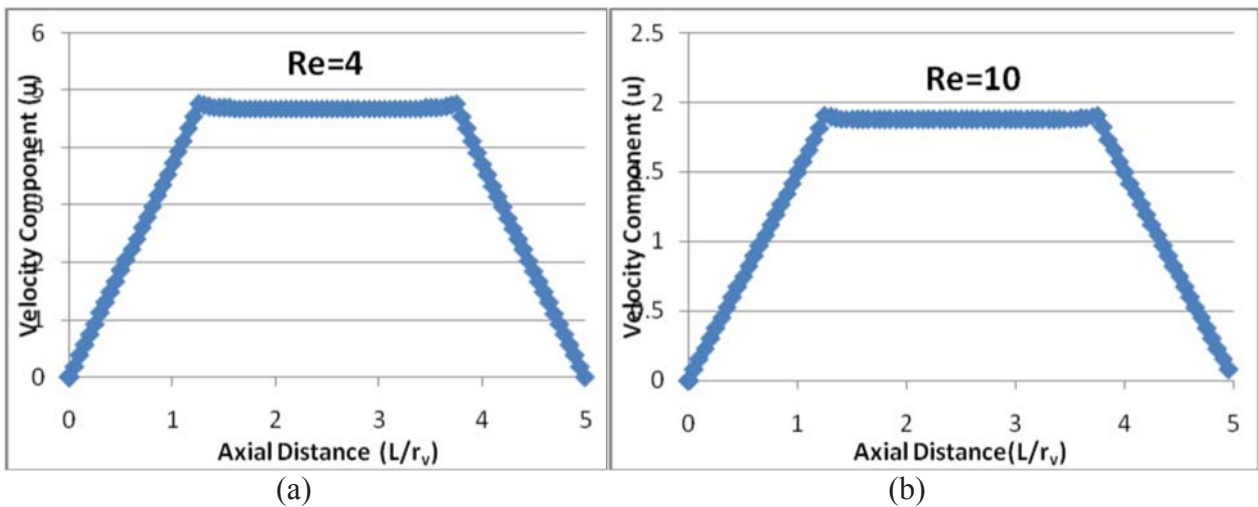


Fig. (5) Distribution of axial velocity at the wall a) $Re = 4$ b) $Re = 10$

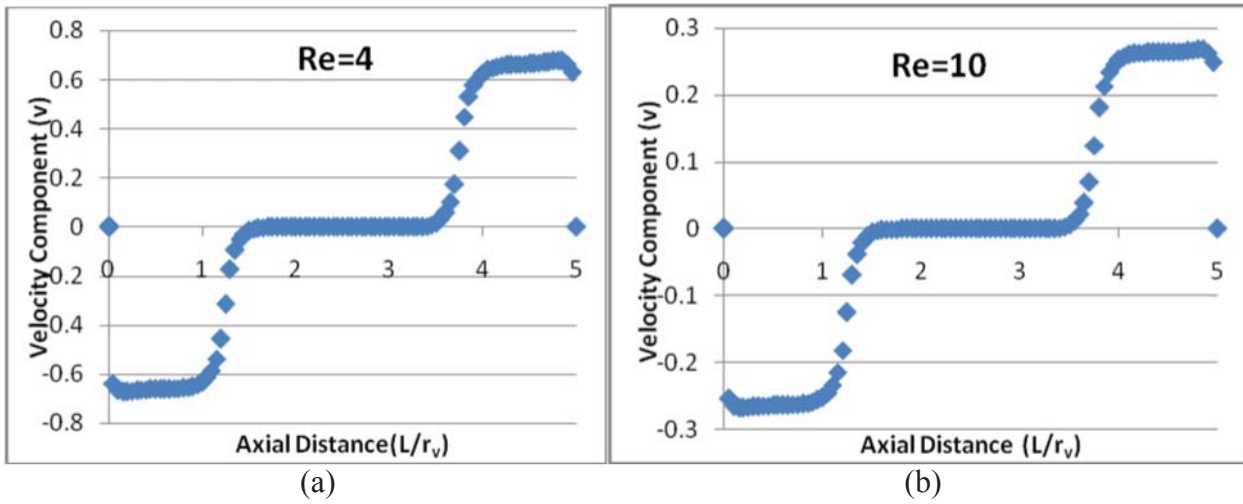


Fig. (6) Distribution of radial velocity at the wall a) Re = 4 b) Re = 10

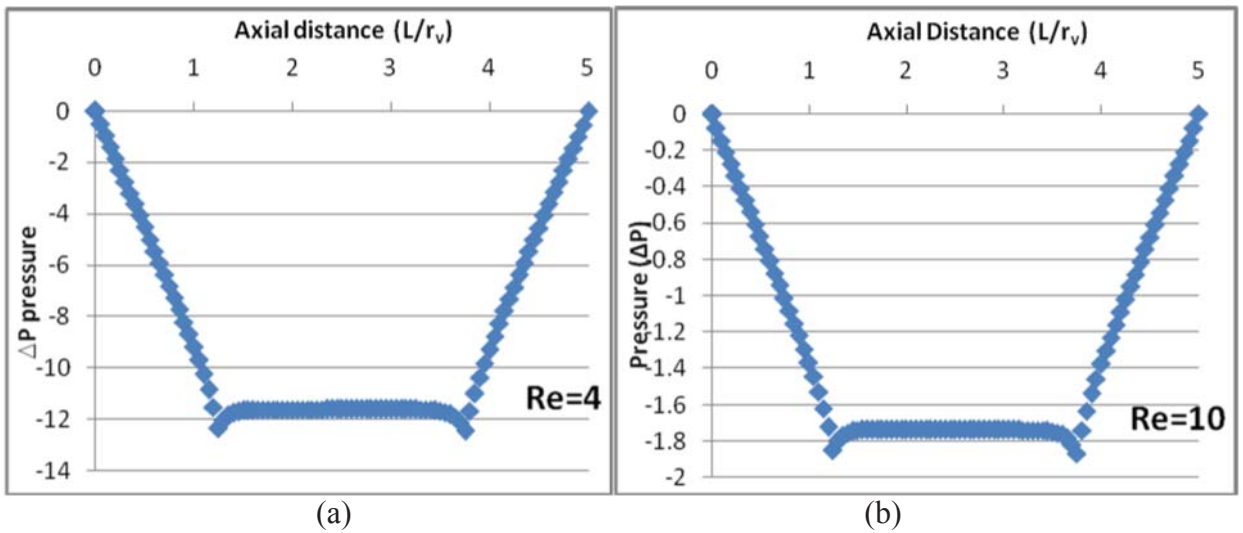


Fig. (7) Pressure distribution at the wall a) Re = 4 b) Re = 10

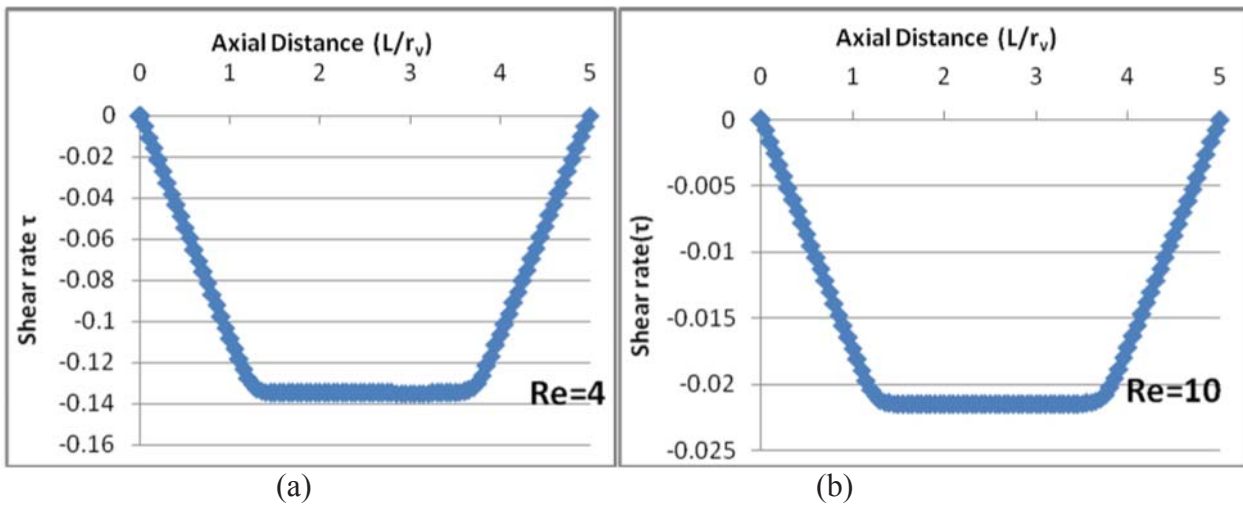


Fig. (8) Distribution of shear rate at the wall a) Re = 4 b) Re = 10

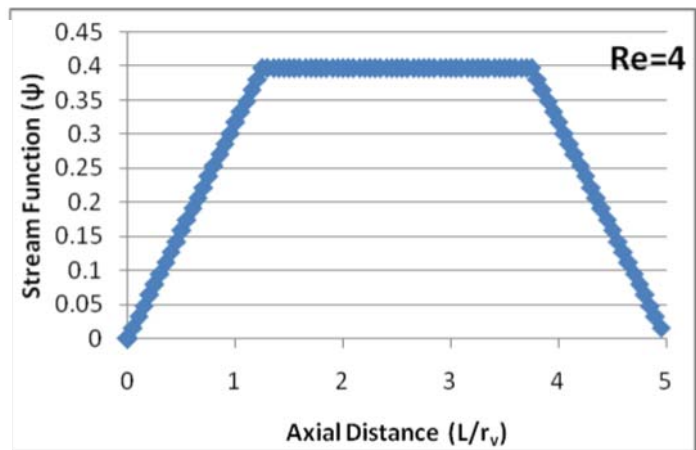
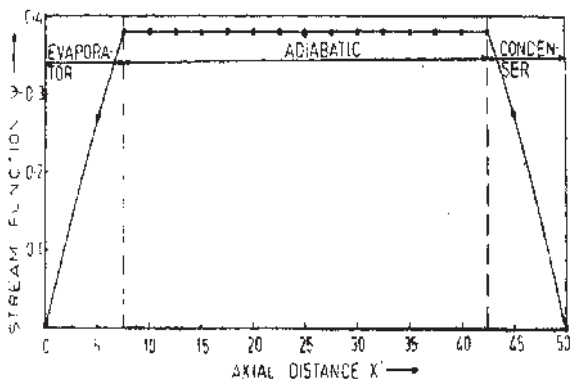


Fig. (9) The stream function calculated in this study versus that of (Rajashree and Sankara, 1990), at the wall for ($Re = 4$)